SIMULATING POTENTIAL STORM SURGES FROM SUPER TYPHOON DOKSURI (2023) IN NORTHERN PHILIPPINES

Justin Joseph Valdez[1] and Tomoya Shibayama[2,3]

In late July of 2023, Super Typhoon Doksuri (local name: Egay) hit the northern part of the Philippines with a peak intensity of 185 km/h and 925 hPa. Storm surges were expected to occur in the area with Doksuri making a direct hit and staying over the Babuyan group of islands. However, no official measurements of surge levels were known to be reported. Thus, there is a need to investigate how high the storm surges could have been on these islands using numerical models. The WRF-FVCOM weather-surge models were used to simulate Doksuri and its potential storm surge at the islands. Although the simulated peak intensities are within good agreement with the observed data, the track deviated northward as it entered the smallest domain where the islands are located. This resulted in simulated storm surge heights of around 0.21-0.48 meters, which were smaller than expected. Improvements in the simulations, particularly on the downscaling of the typhoon over the small islands, are recommended to further understand the potential storm surges in these islands.

Keywords: Typhoon Doksuri; storm surge; numerical modeling; Philippines

INTRODUCTION

In late July of 2023, Super Typhoon Doksuri (local name: Egay) hit the northern part of the Philippines with a peak intensity of 185 km/h and 925 hPa within the Philippine Area of Responsibility (PAGASA, 2023). Doksuri landed twice in the Philippines: first at Fuga island on 25 July 2023 19:10 UTC, then at Dalupiri island approximately 6 hours later. Storm surge warnings were imposed in the northern Philippines, including the provinces of Cagayan, Batanes, Isabela, and Ilocos Norte, prompting residents to evacuate. Doksuri also intensified the rain in mainland Luzon by enhancing the southwest monsoon.

The Babuyan group of islands (Figure 1), part of the Cagayan province, is vulnerable to storm surges of up to 2.00 m under Super Typhoon Haiyan strength (Lapidez et al., 2015). Storm surges were expected to occur in the area with Doksuri making a direct hit and staying over the Babuyan group of islands. However, no official measurements of surge levels were known to be reported. Thus, there is a need to investigate how high the storm surge could have been on these islands, if any. With the difficulty of traveling to the isolated areas such as the Babuyan group of islands in time for field measurements, a numerical modelling of the potential storm surges was performed.

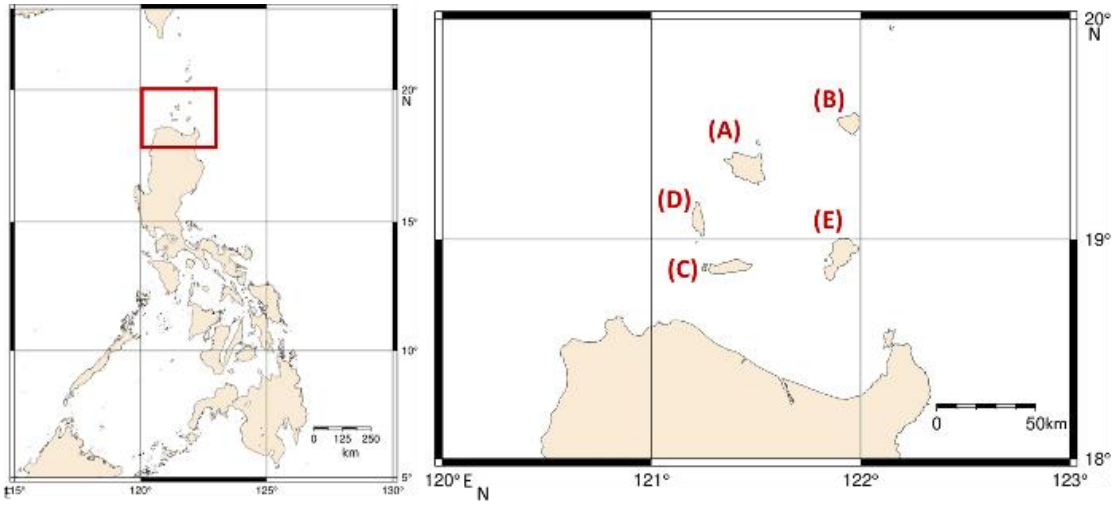

Figure 1. The Babuyan group of islands comprising of (a) Calayan, (b) Babuyan, (c) Fuga, (d) Dalupiri, and (e) Camiguin.

METHODOLOGY

A weather-surge numerical methodology was used in this study, as shown in Figure 2. This modelling set-up has been used in hindcasting tropical cyclones and storm surges in several case

[1] University of the Philippines Diliman, Quezon City, Philippines.
[2] Chuo University, Tokyo, Japan.
[3] Chuo University, Tokyo. Japan.

studies, such as the 2013 Super Typhoon Haiyan at Tacloban in central Philippines (Nakamura et al., 2016; Valdez et al., 2023).

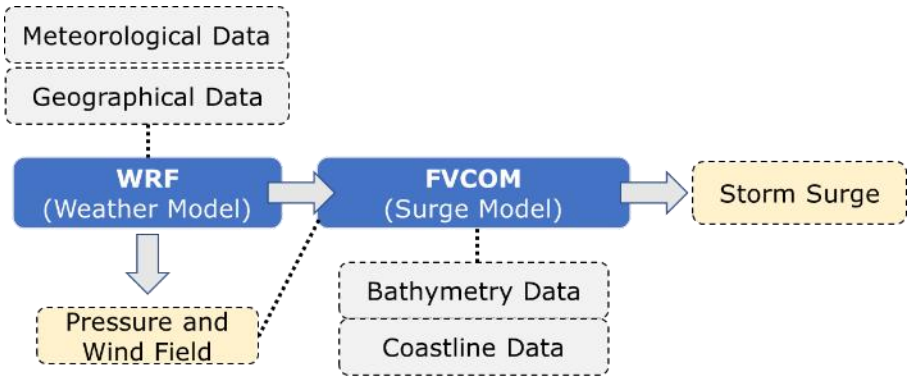

Figure 2. Numerical models used in this study.

Weather Model Numerical Set-up

The Weather Research and Forecasting (WRF) Model (Skamarock et al. 2008) was developed by the National Center for Atmospheric Research (NCAR) and is used to simulate tropical cyclones. Its advantage comes from its versatility to use different physics options to suit the desired simulation. A parent domain (d01) with a grid size of 9 km by 9 km covering the track of Doksuri from its early formation at the Pacific Ocean until its departure from the Philippines was set-up (Figure 3). Additionally, a smaller 3 km by 3 km nested domain (d02) covering the upper half of Luzon and 1 km x 1 km nested domain (d03) focusing on the Babuyan Islands was used with two-way nesting.

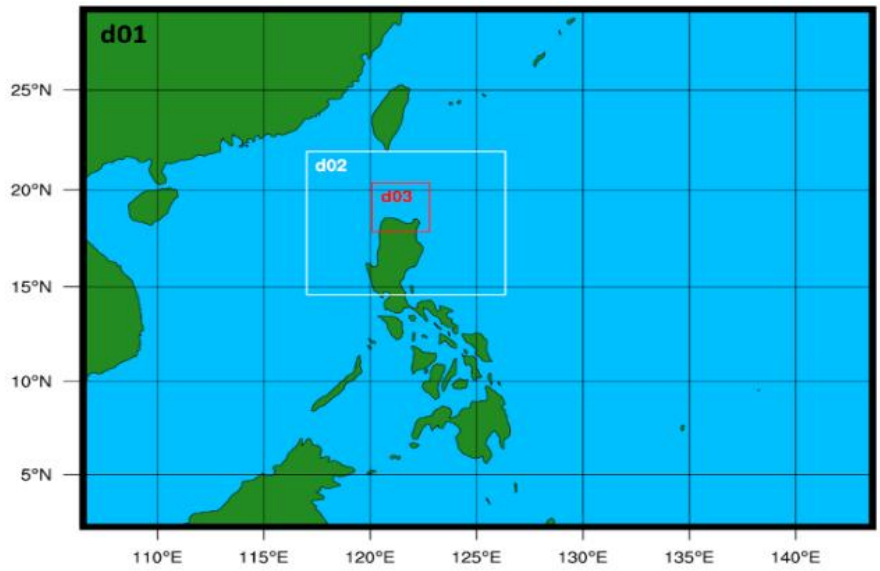

Figure 3. WRF domain set-up for typhoon simulation.

The total simulation period was from 23 July 2023 00:00 to 28 July 2023 00:00 Universal Coordinated Time (UTC) with the the ERA5 meteorological dataset, the latest European Centre for Medium-Range Weather Forecast (ECMWF) reanalysis, as atmospheric input. The domain configuration and selected microphysics in this simulation is listed in Table 1. The simulation time step was set to 30 seconds.

Table 1. WRF Domain Set-up.

	Domain 1 (Parent)	Domain 2 (Nest)	Domain 3 (Nest)
Simulation Start (UTC)	2023-07-23_00:00:00	2023-07-24_00:00:00	2023-07-25_00:00:00
Simulation End (UTC)	2023-07-28_00:00:00	2023-07-27_12:00:00	2023-07-27_00:00:00
Parent Grid Ratio	1	3	3

Grid Spacing (x-direction)	9000 m	3000 m	1000 m
Grid Spacing (y-direction)	9000 m	3000 m	1000 m
Vertical layers	71	71	71
Microphysics	WRF Single-Moment 3-class scheme (WSM3) - Hong et al. 2003		
Longwave and Shortwave Radiation	Rapid Radiative Transfer Model for General Circulation Models Applications (RRTMG) - Iacono et al. 2008		
Surface Layer	Quasi-Normal Scale Elimination (QNSE) surface layer - Sukoriansky et al. 2005		
Land Surface	Noah-Multi-Physics (Noah-MP) land surface model - Niu et al. 2011		
Planetary Boundary Layer	QNSE planetary boundary layer - Sukoriansky et al. 2005		
Cumulus Parametrization	Grell-Freitas (GF) scheme - Grell and Freitas 2014		

Storm Surge Model Numerical Set-up

Using the output pressure and wind fields from WRF, the Finite Volume Community Ocean Model (FVCOM) was used for the storm surge simulation. The FVCOM is a unstructured-grid, three-dimensional primitive equation free-surface coastal ocean model (Chen et al. 2003) that has been applied in several storm surge simulation researches (Ohira et al. 2012; Tasnim 2014; Nakamura et al. 2016). The model uses the finite-volume approach, utilizing the geometric flexibility of the finite element method and computational efficiency of the finite difference method. The governing momentum, continuity, temperature, salinity, and density equations without snow and ice are:

$$\frac{\partial u}{\partial t} + u\frac{\partial u}{\partial x} + v\frac{\partial u}{\partial y} + w\frac{\partial u}{\partial z} - fv = -\frac{1}{\rho_o}\frac{\partial (p_H + p_a)}{\partial x} - \frac{1}{\rho_o}\frac{\partial q}{\partial x} + \frac{\partial}{\partial z}\left(K_m \frac{\partial u}{\partial z}\right) + F_u \quad (1)$$

$$\frac{\partial v}{\partial t} + u\frac{\partial v}{\partial x} + v\frac{\partial v}{\partial y} + w\frac{\partial v}{\partial z} - fu = -\frac{1}{\rho_o}\frac{\partial (p_H + p_a)}{\partial y} - \frac{1}{\rho_o}\frac{\partial q}{\partial y} + \frac{\partial}{\partial z}\left(K_m \frac{\partial v}{\partial z}\right) + F_v \quad (2)$$

$$\frac{\partial w}{\partial t} + u\frac{\partial w}{\partial x} + v\frac{\partial w}{\partial y} + w\frac{\partial w}{\partial z} = -\frac{1}{\rho_o}\frac{\partial q}{\partial z} + \frac{\partial}{\partial z}\left(K_m \frac{\partial w}{\partial z}\right) + F_w \quad (3)$$

$$\frac{\partial u}{\partial x} + \frac{\partial v}{\partial y} + \frac{\partial w}{\partial z} = 0 \quad (4)$$

$$\frac{\partial T}{\partial t} + u\frac{\partial T}{\partial x} + v\frac{\partial T}{\partial y} + w\frac{\partial T}{\partial z} = \frac{\partial}{\partial z}\left(K_h \frac{\partial T}{\partial z}\right) + F_T \quad (5)$$

$$\frac{\partial S}{\partial t} + u\frac{\partial S}{\partial x} + v\frac{\partial S}{\partial y} + w\frac{\partial S}{\partial z} = \frac{\partial}{\partial z}\left(K_h \frac{\partial S}{\partial z}\right) + F_S \quad (6)$$

$$\rho = \rho(T, S, p) \quad (7)$$

where x, y, and z are the east, north, and vertical axes in the Cartesian coordinate system; u, v, and w are the directional velocity components; T is the temperature; S is the salinity; ρ is the density; p_a is the sea surface air pressure; p_H is the hydrostatic pressure; q is the non-hydrostatic pressure; f is the Coriolis parameter; g is the gravitational acceleration; K_m is the vertical eddy viscosity coefficient; and K_h is the thermal vertical eddy diffusion coefficient. At the right-hand side of the equations, F_u, F_v, F_T, and F_S are the horizontal momentum, thermal, and salt diffusion terms, respectively.

Table 2 summarizes the domain configuration for the FVCOM storm surge simulation. An unstructured mesh domain of 153,361 nodes and 304,728 triangular elements was set up over the seas surrounding the five islands (Figure 4) with the General Bathymetric Chart of the Oceans (GEBCO) 2023 grid as the bathymetry data. The coastline data from the Global Self-consistent, Hierarchical, High-resolution Geography (GSHHG) Version 2.3.7 Database (Wessel and Smith 1996) was used for the islands. Tides were not included in the modelling to focus more on the storm surge brought by Doksuri to focus more on the storm surge component.

Table 2. FVCOM Domain Set-up.	
Simulation Start (UTC)	2023-07-25_00:00:00
Simulation End (UTC)	2023-07-27_00:00:00
Number of Nodes	153,361
Mesh sizes	1000 m (open boundary to 5 m (islands)

Number of Elements	304,728
Coastline Data	GSHHG Version 2.3.7 Database (Full Resolution; Level 1)
Bathymetry Data	GEBCO 2023 30-arc second grid

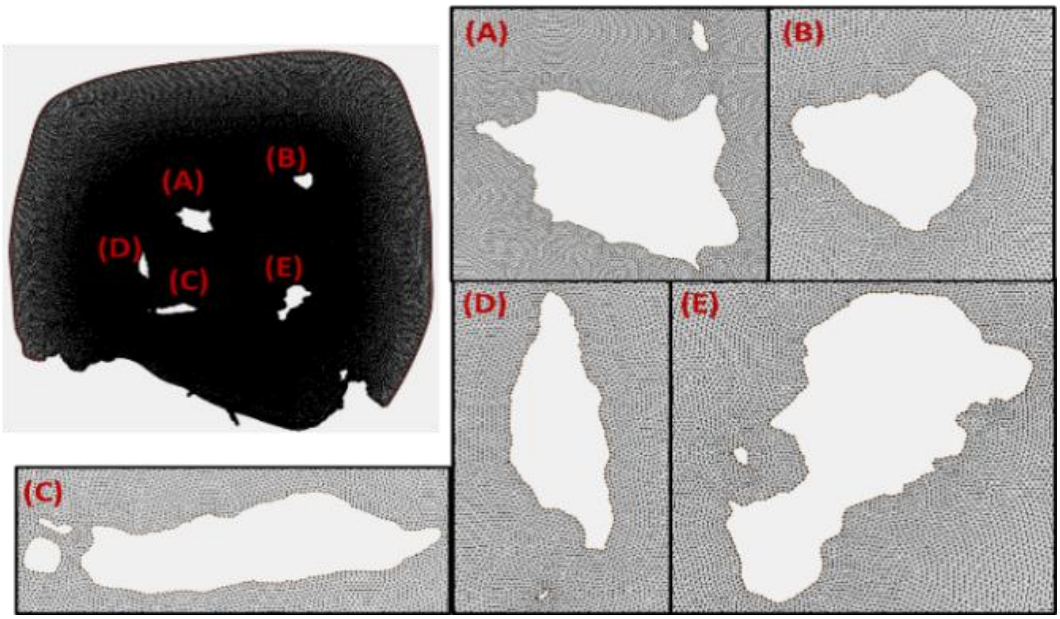

Figure 4. FVCOM domain set-up for storm surge simulation, with zoom-in of the five islands: (a) Calayan, (b) Babuyan, (c) Fuga, (d) Dalupiri, and (e) Camiguin.

The drag coefficient C_D was computed based on the momentum transfer equations from Honda and Mitsuyasu (1980) and Yokota et al. (2011):

$$C_D = \begin{cases} 0.00128(1 - 0.01890w) & w \leq 8.0\ m/s \\ 0.000581(1 + 0.1078w) & 8.0\ m/s\ < w \leq 30\ m/s \\ 0.00246 & w > 30\ m/s \end{cases} \quad (8)$$

where w is the wind speed (m/s). This was the wind drag coefficient used by Nakamura et al. (2016) and Valdez et al. (2023) in the Typhoon Haiyan simulation at Leyte. The change in water level at select points near the coast of each island was graphed and the peak surge heights were noted.

RESULTS AND DISCUSSION

Typhoon Simulation

The WRF simulated typhoon intensities, mean sea level pressure (MSLP) and maximum wind speeds, are shown in Figure 5. Using the selected microphysics from the sensitivity analysis, the intensity results showed good agreement with the observed data, with peak pressure and wind deviations of 3.80 hPa and 1.65 m/s, respectively. However, it was noted that the simulated MSLP and maximum wind speeds at the observed peak time of the typhoon (around 26 July 2023 UTC) were much lower than expected. The simulated pressure field (Figure 6) shows that the simulated typhoon was already passing over the Babuyan islands, which could have weakened its intensity. Also, the simulated typhoon made landfall at Babuyan island instead of Dalupiri and Fuga islands, shifting the track northeastward.

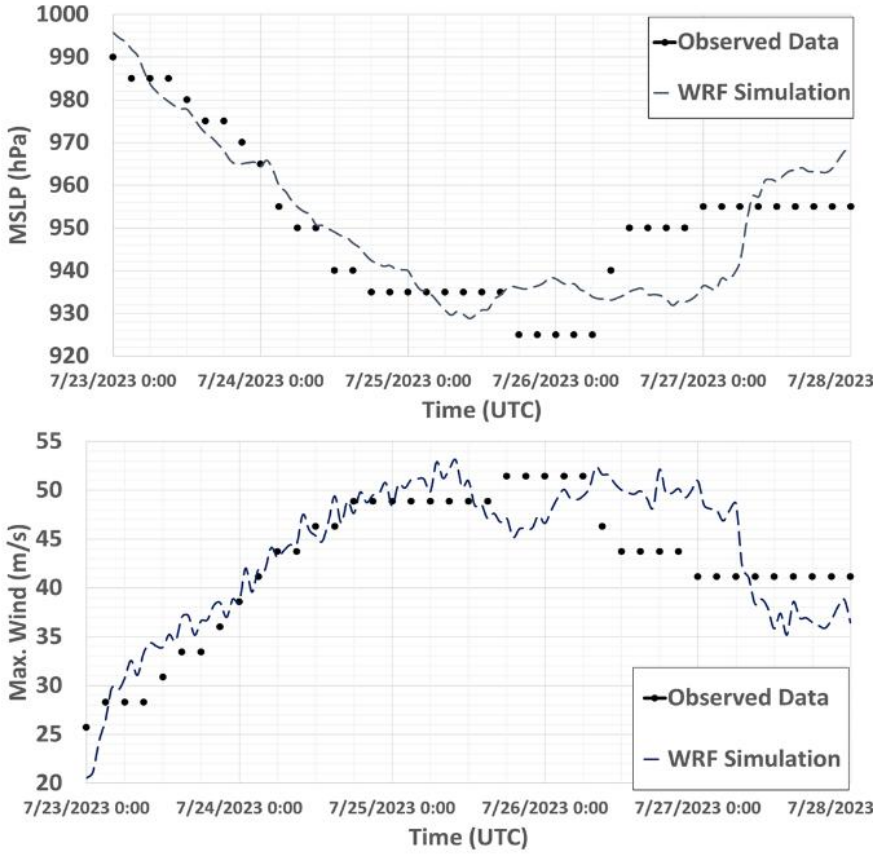

Figure 5. MSLP (above) and max. wind speeds (below).

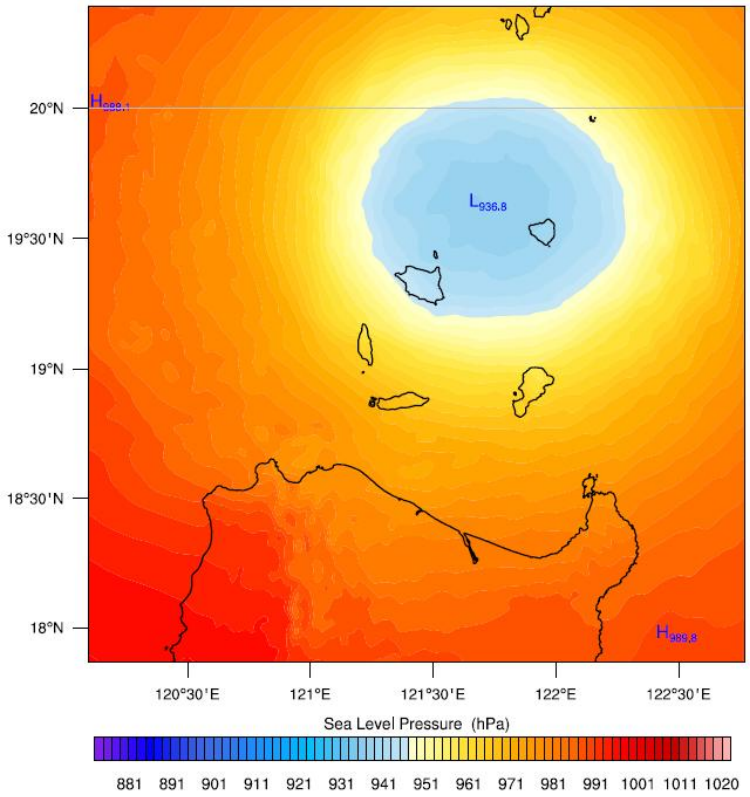

Figure 6. WRF simulated wind field over the Babuyan islands (domain d03) on 26 July 2023 UTC.

The simulated typhoon track (Figure 7) also agreed with the observed data as it approached the Philippines. However, the simulated track slowly deviated as it moved towards the domain d03, where the Babuyan islands are located. Acknowledging the gradual discrepancy of the track, it was still deemed worthwhile to investigate the possibility of storm surge occurring at the islands under the simulated intensities and track of Doksuri.

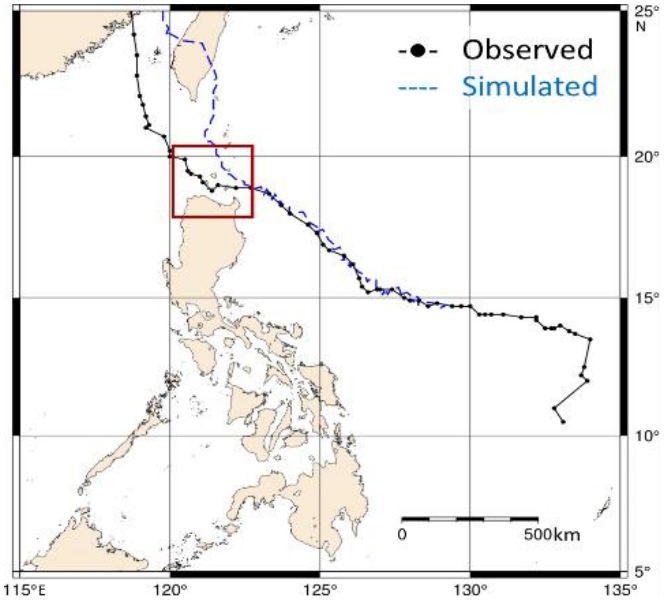

Figure 7. Comparison of typhoon tracks.

Storm Surge Simulation

Using the pressure and wind field results from the WRF, the simulated storm surges from the FVCOM for each of the five islands are graphed in Figure 8. It can be seen that the surge reached 0.31 m, 0.31 m, 0.21 m, 0.23 m, and 0.48 m at Calayan, Babuyan, Fuga, Dalupiri, and Camiguin islands, respectively. The started to arrive at around 25 July 2025 12:00 UTC, when the simulated typhoon entered domain d03. Camiguin Island, the easternmost part of the group of islands, had the earliest and largest peak storm surge height. The other four islands (Calayan, Babuyan, Fuga, and Dalupiri) had similar storm surge arrival and peak trends. It is noted that the peak surges are lower than expected due to the shift in the typhoon track, and consequently the wind field, over the islands.

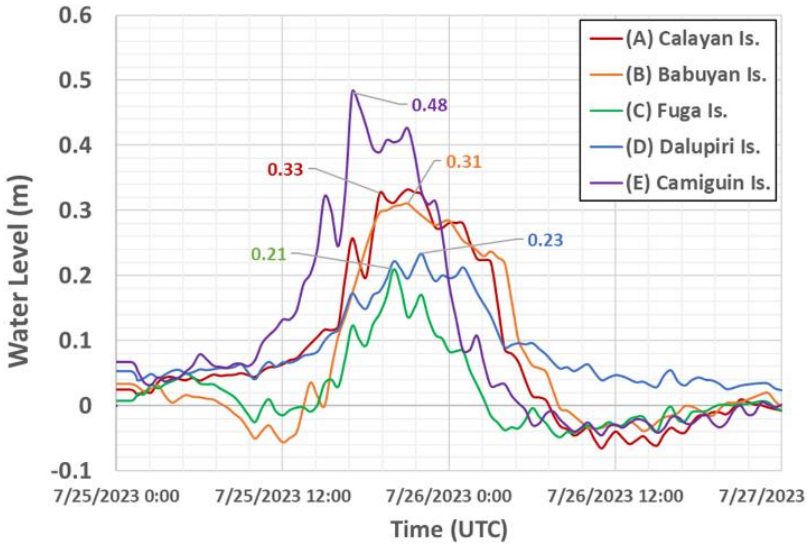

Figure 8. Comparison of simulated storm surges at the five islands.

Under the simulated intensities of Super Typhoon Doksuri, which were in good agreement with recorded data, potential storm surges were calculated at each of the five islands in the study area. However, the deviated typhoon track from the simulation could have shifted the surges within the area. Noting that Doksuri was observed to make landfall at Fuga and Dalupiri islands, which had the two lowest storm surges in the simulated results, a more accurate typhoon track simulation could produce an even higher potential surge in these islands. The results showed that even if the simulated intensities of the typhoon are within acceptable ranges, deviation in the simulated track (and consequently the wind field over the study area) significantly affects the expected storm surge heights of the model.

Nonetheless, it is important to acknowledge the limitations of the present results and aim for an improved simulation result to verify the potential storm surges. Downscaling the typhoon in WRF was difficult, as the track deviation started as the simulated typhoon entered the smallest domain (see Figure 7), thus this could be the focus for improvement. It is recommended to adjust the domain set-up in WRF, such as potentially removing domain d03 for reducing errors in downscaling and exploring other physics options (those used in other typhoon simulations in the Philippines).

Even if the potential storm surges (0.21-0.48 m) were not as high as those from Typhoon Haiyan at Tacloban (as high as 6 m), there is still utmost importance of documenting these events for disaster preparedness strategies such as surge hazard maps, building back better, and evacuation planning.

CONCLUSION

The numerical modeling showed that potential storm surges of up to 0.48 m could have occurred in the northern Philippines, particularly at the Babuyan group of islands due to the 2023 Super Typhoon Doksuri. The typhoon intensities (pressure and wind) were simulated well using the WRF model. However, there was a deviation in the typhoon track which could have shifted the peak surges in the area simulated in the FVCOM model. Improvements in the simulations, particularly on the typhoon, are recommended to further understand the potential storm surges in these islands. By using the improved model, it will be possible to send caution to the residents to evacuate on time.

ACKNOWLEDGMENTS

The author acknowledges the Office of the Chancellor and the University of the Philippines Diliman, through the Office of the Vice Chancellor for Research and Development, for funding support through the PhD Incentive Grant 242417 PhDIA YEAR 1. Additionally, the JSPS KAKENHI Grant Number JP20KK0107 supported this work.

REFERENCES

Chen, C., Liu, H., and Beardsley, R. 2003. An Unstructured Grid, Finite-Volume Three-Dimensional, Primitive Equations Ocean Model: Application to Coastal Ocean and Estuaries, *Journal of Atmospheric and Oceanic Technology*, 20, 159-186.

Grell, G. and Freitas, S. 2014. A scale and aerosol aware stochastic convective parameterization for weather and air quality modeling, *Atmos. Chem. Phys.*, 14, 5233‑5250.

Honda, C., and Mitsuyasu, K. 1980. Laboratory study on wind effect to ocean surface, *J Coast Eng JSCE*, 27, 90-93.

Hong, S., Dudhia, J., and Chen, S. 2004. A Revised Approach to Ice Microphysical Processes for the Bulk Parameterization of Clouds and Precipitation, *Monthly Weather Review*, 132, 103-120.

Iacono, M., Delamere, J., Mlawer, E., Shepard, M., Clough, S., and Collins, W. 2008. Radiative forcing by long-lived greenhouse gases: Calculations with the AER radiative transfer models, *J. Geophys. Res.*, 113, D13103.

Lapidez, J.P., Tablazon, J., Dasallas, L., Gonzalo, L.A., Cabacaba, K.M., Ramos, M.M.A., Suarez, J.K., Santiago, J., Lagmay, A.M.F., and Manalo, V. 2015. Identification of storm surge vulnerable areas in the Philippines through the simulation of Typhoon Haiyan-induced storm surge levels over historical storm tracks, *Nat. Hazards Earth Syst. Sci.*, 15, 1473-1481.

Nakamura, R., Shibayama, T., Esteban, M., and Iwamoto, T. 2016. Future typhoon and storm surges under different global warming scenarios: case study of typhoon Haiyan (2013), *Natural Hazards*, 82, 1645-1681.

Niu, G., Yang, Z., Mitchell, K., Chen, F., Ek, M., Barlage, M., Kumar, A., Manning, K., Niyogi, D., Rosero, E., Tewali, M., and Xia, Y. 2011. *The community Noah land surface model with multiparameterization options (Noah-MP): 1. Model description and evaluation with local-scale measurements*, J. Geophys. Res., 116, D12109.

Ohira, K., Shibayama, T., and Esteban M. 2012. Forecasting Change of Wave and Storm Surge Damage caused by Typhon Affected by Climate Change-Development of Meteorology-Wave-Storm Surge-Tide Coupled Model and Long Term Prediction, *J Jpn Soc Civil Eng Ser B2*, 68, I_291-I_295.

PAGASA. 2023. Tropical Cyclone Preliminary Report – Super Typhoon Egay (Doksuri), *Philippine Atmospheric, Geophysical and Astronomical Services Administration,* Philippines.

Skamarock, W., Klemp, J., Dudhia, J., Gill, D., Barker, D., Duda, M., Huang, X., Wang, W., and Powers J. 2008. A Description of the Advanced Research WRF Version 3, *NCAR Technical Note*.

Sukoriansky, S., Galerpin, B., and Perov, V. 2005. Application of a New Spectral Theory of Stably Stratified Turbulence to the Atmospheric Boundary Layer over Sea Ice, *Boundary-Layer Meteorology*, 117, 231-257.

Tasnim, K. 2014. Numerial Simulation of Cyclonic Storm Surges Over the Bay of Bengal Using a Meteorology-Wave-Surge-Tide Coupled Model, *Coastal Engineering Proceedings*, 1, 26.

Valdez, J., Shibayama, T., Takabatake, T., and Esteban, M. 2023. Simulated flood forces on a building due to the storm surge by Typhoon Haiyan, *Coastal Engineering Journal*, 65, 21-38.

Wessel, P., and Smith, W. 1996. A global, self-consistent, hierarchical, high-resolution shoreline database, *JGR Solid Earth*, 101, 8741-8743.

Yokota, M., Hashimoto, N., Tanaka, Y., and Hodama, M. 2011. Dependence property of the distance from the strong wind area to the wave observation station in the inverse estimation of sea surface drag coefficient, *J Jpn Soc Civil Eng Ser B*, 67, 903-907.